

# Symmetric-conservative metric evaluations for higher-order finite difference scheme with the GCL identities on three-dimensional moving and deforming mesh

Y. Abe\*, N. Iizuka\*\*, T. Nonomura\*\*\*, K. Fujii\*\*\*  
Corresponding author: abe@flab.isas.jaxa.jp

\*Department of Aeronautics and Astronautics, University of Tokyo, Japan.

\*\*Institute of Industrial Science, University of Tokyo, Japan.

\*\*\*Institute of Space and Astronautical Science, JAXA, Japan.

**Abstract:** New conservative forms are introduced for time metrics and the Jacobian, which satisfy the geometric conservation law (:GCL) identity even when higher-order spatial discretization is employed for the moving and deforming meshes. The conservative quantities are ensured to keep constant for three-dimensional moving and deforming meshes with use of these new forms for the computation of the uniform flow. In addition, one of the new forms has spatial symmetry property, and some tests indicate the significance of the spatial symmetry in the expression of time metrics and the Jacobian.

*Keywords:* geometric conservation law, volume conservation law, body-fitted coordinates, freestream preservation, vortex preservation, moving and deforming grid.

## 1 Introduction

Body-fitted coordinate systems are often adopted to compute the fluid motion around arbitrary body shapes. In this case, the coordinate transformation metrics from the body-fitted coordinate system to the Cartesian coordinate system are introduced for the computation. Although transformation metrics analytically satisfy freestream preservation, which is called the “geometric conservation law” (GCL) [11], some discretized forms of metrics break the GCL identities with certain finite difference schemes. The GCL identities consist of “surface closure law” (SCL) <sup>1</sup> and “volume conservation law” (VCL) [17]. We focus on the VCL identity. For details on the GCL identities, refer to the review article [12][13].

In terms of the freestream preservation for a moving and deforming grid, Visbal and Gaitonde have proposed a method to replace the governing equation with an equation in which the time derivative of the Jacobian is split from the conservative fluxes (Sec. 3.3 in [16] and Sec. 4.3 in [15]) for high-order schemes; this is called the *split form* in this paper; on the other hand, the conservative expression of the governing equation is referred to as the *conservative form*. In the *split form*, the error within the discretized VCL identity is subtracted and the freestream is preserved. However, the *split form* is potentially nonconservative in terms of the time derivative of the Jacobian, whose inverse corresponds to each cell volume in the computation. As a result, the summation of conservative quantities in the computational region is not preserved when the computational region is being deformed. The use of the *conservative form* of the governing equation cancels out the error related to the preservation of conservative quantities, where the discretized VCL identities should be satisfied for freestream preservation. A number of techniques for the discretization of time metrics and the Jacobian have been proposed from a geometric viewpoint, e.g., finite volume schemes [13], which are not suitable for high-order finite difference schemes. In addition, the special form (Sec. 3.D in [10]) has

---

<sup>1</sup>This identity is called “surface (area) conservation law” in previous studies [4][14][17]. It is called “surface closure law” in this paper and states that the sum of surface area vectors equals 0.

been proposed, in which the conservative flux for a freestream condition is subtracted from the *conservative form* in advance. However, this method is not valid for a flow field where the freestream cannot be defined.

We aim to propose new analytical forms for time metrics and the Jacobian, that is, *asymmetric conservative metrics* and *symmetric conservative metrics* of which discretizations satisfy the VCL identity at each time step of any linear high-order finite difference scheme. The use of *asymmetric* and *symmetric conservative metrics* for time metrics and the Jacobian enables adopting the *conservative form* of the governing equation. Therefore, it is expected that the preservation of both the freestream and conservative quantities that are integrated over the computational region is accomplished for any linear high-order finite difference scheme. Note that a form of *asymmetric conservative metrics* has been proposed for the discretization of spatial metrics for stationary grids [11]. In terms of coordinate invariance, spatial symmetry property has been introduced to *asymmetric conservative metrics* for spatial metrics [14]. These discretized spatial metrics satisfy the SCL identities for any linear high-order finite difference scheme, which has been experimentally proven by Visbal and Gaitonde [15] and mathematically proven by Vinokur and Yee [14]. Nonlinear high-order schemes are addressed in [4][8]. It should be mentioned that for moving but nondeforming grid, the use of *nonconservative metrics* for time metrics and the Jacobian can satisfy the VCL identity for any linear high-order finite difference scheme, and so has been constructed by Vinokur and Yee [14]. The forms proposed here, i.e., *asymmetric* and *symmetric conservative metrics* for time metrics and the Jacobian are an extension of those used for spatial metrics [15][14].

The rest of the paper is organized as follows. We state the problem and assumptions in Sec. 2. The newly proposed analytical expression, i.e., *asymmetric* and *symmetric conservative metrics* for time metrics and the Jacobian are introduced, and its validation for any linear high-order finite difference scheme is shown in Sec. 3. Numerical tests on three-dimensional deforming grids with high-order schemes are described in terms of freestream preservation and the resolution of an isentropic vortex in Sec. 4. These numerical tests also validate the *conservative form* of the governing equation in terms of the preservation of conservative quantities integrated over the computational region. We summarize the results and state our future work relating to the proposed forms in Sec. 5.

## 2 Coordinate system and governing equation

Consider the flow field around an arbitrary body shape, where the Cartesian and body-fitted coordinate systems are introduced to represent physical space. Let the Cartesian coordinate system be  $\{t, x, y, z\}$  and the body-fitted coordinate system be  $\{\tau, \xi, \eta, \zeta\}$ . Each coordinate is assumed to have the following relationships:

$$\xi = \xi(t, x, y, z), \quad \eta = \eta(t, x, y, z), \quad \zeta = \zeta(t, x, y, z), \quad (1)$$

$$x = x(\tau, \xi, \eta, \zeta), \quad y = y(\tau, \xi, \eta, \zeta), \quad z = z(\tau, \xi, \eta, \zeta), \quad (2)$$

$$t = \tau, \quad (3)$$

where  $\{t, x, y, z\}$  are assumed to be nondimensionalized by the reference time and length. The coordinate transformation matrix is defined from the Cartesian coordinate system to the body-fitted coordinate system. The spatial metrics are defined as

$$\xi_z/J = x_\eta y_\zeta - x_\zeta y_\eta, \quad \eta_z/J = x_\zeta y_\xi - x_\xi y_\zeta, \quad \zeta_z/J = x_\xi y_\eta - x_\eta y_\xi, \quad (4)$$

where  $\zeta_z$  denotes the partial derivative of  $\zeta$  in terms of  $z$ , i.e.,  $\partial\zeta/\partial z$ . The partial derivatives of  $\tau$ ,  $\xi$ ,  $\eta$ ,  $\zeta$ ,  $t$ ,  $x$ , and  $y$  are similarly denoted in the note. The Jacobian  $J$  is defined as

$$\begin{aligned} & \text{(Non-cons-met.)} \\ 1/J & \equiv \frac{\partial(x, y, z)}{\partial(\xi, \eta, \zeta)} = x_\xi y_\eta z_\zeta - x_\eta y_\xi z_\zeta + x_\zeta y_\xi z_\eta - x_\xi y_\zeta z_\eta + x_\eta y_\zeta z_\xi - x_\zeta y_\eta z_\xi, \end{aligned} \quad (5)$$

where (*Non-cons-met.*) denotes the *nonconservative metric*. The time metrics are defined as

$$(\text{Non-cons-met.}) \quad \xi_t/J = x_\eta y_\tau z_\zeta - x_\eta y_\zeta z_\tau + x_\zeta y_\eta z_\tau - x_\zeta y_\tau z_\eta + x_\tau y_\zeta z_\eta - x_\tau y_\eta z_\zeta, \quad (6)$$

$$(\text{Non-cons-met.}) \quad \eta_t/J = x_\xi y_\zeta z_\tau - x_\xi y_\tau z_\zeta + x_\zeta y_\tau z_\xi - x_\zeta y_\xi z_\tau + x_\tau y_\xi z_\zeta - x_\tau y_\zeta z_\xi, \quad (7)$$

$$(\text{Non-cons-met.}) \quad \zeta_t/J = x_\eta y_\xi z_\tau - x_\eta y_\tau z_\xi + x_\xi y_\tau z_\eta - x_\xi y_\eta z_\tau + x_\tau y_\eta z_\xi - x_\tau y_\xi z_\zeta. \quad (8)$$

The other metrics are similarly introduced, but their definitions are not presented here. The compressible Euler equations are written in the body-fitted coordinate system as

$$\hat{Q}_\tau = -\hat{E}_\xi - \hat{F}_\eta - \hat{G}_\zeta, \quad (9)$$

$$\hat{Q} = \frac{1}{J} \begin{bmatrix} \rho \\ \rho u \\ \rho v \\ \rho w \\ e \end{bmatrix}, \quad \hat{E} = \frac{1}{J} \begin{bmatrix} \rho U \\ \rho u U + \xi_x p \\ \rho v U + \xi_y p \\ \rho w U + \xi_z p \\ (e+p)U - \xi_t p \end{bmatrix}, \quad \hat{F} = \frac{1}{J} \begin{bmatrix} \rho V \\ \rho u V + \eta_x p \\ \rho v V + \eta_y p \\ \rho w V + \eta_z p \\ (e+p)V - \eta_t p \end{bmatrix}, \quad \hat{G} = \frac{1}{J} \begin{bmatrix} \rho W \\ \rho u W + \zeta_x p \\ \rho v W + \zeta_y p \\ \rho w W + \zeta_z p \\ (e+p)W - \zeta_t p \end{bmatrix},$$

$$U = \xi_t + \xi_x u + \xi_y v + \xi_z w,$$

$$V = \eta_t + \eta_x u + \eta_y v + \eta_z w,$$

$$W = \zeta_t + \zeta_x u + \zeta_y v + \zeta_z w,$$

where  $\rho, \mathbf{u} = (u, v, w), p$ , and  $e$  denote density, flow velocity vector expressed in Cartesian coordinates, pressure, and whole energy per unit volume, respectively. All variables are normalized by the reference length, density, and sound speed.  $\mathbf{U} = (U, V, W)$  is called the contravariant velocity vector. The equation of state of ideal gas is coupled with Eq.(9) and the equations are closed.

### 3 New evaluation for time metrics and the Jacobian

In this section, we introduce a new evaluation for time metrics and the Jacobian. First, *asymmetric conservative metrics* for time metrics and the Jacobian are introduced. Then, we show how discretized *asymmetric conservative metrics* satisfy the VCL identity for any linear high-order finite difference scheme. Finally, the *symmetric conservative metrics* are proposed from a viewpoint of coordinate invariance property for computation.

#### 3.1 Conservative metrics

Proper discretization of metrics and the Jacobian is often conducted on the basis of freestream preservation, which is called GCL [11]:

$$(\xi_x/J)_\xi + (\eta_x/J)_\eta + (\zeta_x/J)_\zeta = 0, \quad (10)$$

$$(\xi_y/J)_\xi + (\eta_y/J)_\eta + (\zeta_y/J)_\zeta = 0, \quad (11)$$

$$(\xi_z/J)_\xi + (\eta_z/J)_\eta + (\zeta_z/J)_\zeta = 0, \quad (12)$$

$$(1/J)_\tau + (\xi_t/J)_\xi + (\eta_t/J)_\eta + (\zeta_t/J)_\zeta = 0, \quad (13)$$

where Eqs.(10)–(12) are the SCL identities, and Eq.(13) is the VCL identity [17]. The SCL and VCL identities are analytical identities that represent the surface closure and volume conservation of finite volumes [13], respectively. However, note that the discretized SCL and VCL identities are often broken when improper discretization is employed for time metrics and the Jacobian. We propose a new evaluation for time metrics and the Jacobian that satisfies the VCL identity with any linear high-order finite difference scheme. Now,

we let

$$\begin{aligned} & \text{(Asym-cons-met.)} \\ 1/J &= [\underbrace{\{(x_\xi y)_\eta - (x_\eta y)_\xi\}z}_A]_\zeta + [\underbrace{\{(x_\zeta y)_\xi - (x_\xi y)_\zeta\}z}_B]_\eta + [\underbrace{\{(x_\eta y)_\zeta - (x_\zeta y)_\eta\}z}_C]_\xi, \end{aligned} \quad (14)$$

$$\begin{aligned} & \text{(Asym-cons-met.)} \\ \xi_t/J &= [\underbrace{\{(x_\tau y)_\zeta - (x_\zeta y)_\tau\}z}_D]_\eta + [\underbrace{\{(x_\eta y)_\tau - (x_\tau y)_\eta\}z}_E]_\zeta + [\underbrace{\{(x_\zeta y)_\eta - (x_\eta y)_\zeta\}z}_{-C}]_\tau, \end{aligned} \quad (15)$$

$$\begin{aligned} & \text{(Asym-cons-met.)} \\ \eta_t/J &= [\underbrace{\{(x_\tau y)_\xi - (x_\xi y)_\tau\}z}_F]_\zeta + [\underbrace{\{(x_\xi y)_\zeta - (x_\zeta y)_\xi\}z}_{-B}]_\tau + [\underbrace{\{(x_\zeta y)_\tau - (x_\tau y)_\zeta\}z}_{-D}]_\xi, \end{aligned} \quad (16)$$

$$\begin{aligned} & \text{(Asym-cons-met.)} \\ \zeta_t/J &= [\underbrace{\{(x_\eta y)_\xi - (x_\xi y)_\eta\}z}_{-A}]_\tau + [\underbrace{\{(x_\tau y)_\eta - (x_\eta y)_\tau\}z}_{-E}]_\xi + [\underbrace{\{(x_\xi y)_\tau - (x_\tau y)_\xi\}z}_{-F}]_\eta, \end{aligned} \quad (17)$$

where *(Asym-cons-met.)* denotes *asymmetric conservative metrics*. The discretized time metrics and the Jacobian based on Eqs.(14)–(17) always satisfy the VCL identity (13), regardless of the finite difference scheme employed for the discretization under the condition described in Sec. 3.2. In terms of coordinate invariance, we introduce the spatial symmetry property into Eqs.(14)–(17), and get

*(Sym-cons-met.)*

$$\begin{aligned} 1/J &= \left\{ [\{(x_\xi y)_\eta - (x_\eta y)_\xi\}z]_\zeta + [\{(x_\zeta y)_\xi - (x_\xi y)_\zeta\}z]_\eta + [\{(x_\eta y)_\zeta - (x_\zeta y)_\eta\}z]_\xi \right. \\ &+ [\{(y_\xi z)_\eta - (y_\eta z)_\xi\}x]_\zeta + [\{(y_\zeta z)_\xi - (y_\xi z)_\zeta\}x]_\eta + [\{(y_\eta z)_\zeta - (y_\zeta z)_\eta\}x]_\xi \\ &+ [\{(z_\xi x)_\eta - (z_\eta x)_\xi\}y]_\zeta + [\{(z_\zeta x)_\xi - (z_\xi x)_\zeta\}y]_\eta + [\{(z_\eta x)_\zeta - (z_\zeta x)_\eta\}y]_\xi \\ &+ [\{(y_\eta x)_\xi - (y_\xi x)_\eta\}z]_\zeta + [\{(y_\xi x)_\zeta - (y_\zeta x)_\xi\}z]_\eta + [\{(y_\zeta x)_\eta - (y_\eta x)_\zeta\}z]_\xi \\ &+ [\{(z_\eta y)_\xi - (z_\xi y)_\eta\}x]_\zeta + [\{(z_\xi y)_\zeta - (z_\zeta y)_\xi\}x]_\eta + [\{(z_\zeta y)_\eta - (z_\eta y)_\zeta\}x]_\xi \\ &+ [\{(x_\eta z)_\xi - (x_\xi z)_\eta\}y]_\zeta + [\{(x_\xi z)_\zeta - (x_\zeta z)_\xi\}y]_\eta + [\{(x_\zeta z)_\eta - (x_\eta z)_\zeta\}y]_\xi \left. \right\}/6, \end{aligned} \quad (18)$$

*(Sym-cons-met.)*

$$\begin{aligned} \xi_t/J &= \left\{ [\{(x_\tau y)_\zeta - (x_\zeta y)_\tau\}z]_\eta + [\{(x_\eta y)_\tau - (x_\tau y)_\eta\}z]_\zeta + [\{(x_\zeta y)_\eta - (x_\eta y)_\zeta\}z]_\tau \right. \\ &+ [\{(y_\tau z)_\zeta - (y_\zeta z)_\tau\}x]_\eta + [\{(y_\eta z)_\tau - (y_\tau z)_\eta\}x]_\zeta + [\{(y_\zeta z)_\eta - (y_\eta z)_\zeta\}x]_\tau \\ &+ [\{(z_\tau x)_\zeta - (z_\zeta x)_\tau\}y]_\eta + [\{(z_\eta x)_\tau - (z_\tau x)_\eta\}y]_\zeta + [\{(z_\zeta x)_\eta - (z_\eta x)_\zeta\}y]_\tau \\ &+ [\{(y_\zeta x)_\tau - (y_\tau x)_\zeta\}z]_\eta + [\{(y_\tau x)_\eta - (y_\eta x)_\tau\}z]_\zeta + [\{(y_\eta x)_\zeta - (y_\zeta x)_\eta\}z]_\tau \\ &+ [\{(z_\zeta y)_\tau - (z_\tau y)_\zeta\}x]_\eta + [\{(z_\tau y)_\eta - (z_\eta y)_\tau\}x]_\zeta + [\{(z_\eta y)_\zeta - (z_\zeta y)_\eta\}x]_\tau \\ &+ [\{(x_\zeta z)_\tau - (x_\tau z)_\zeta\}y]_\eta + [\{(x_\tau z)_\eta - (x_\eta z)_\tau\}y]_\zeta + [\{(x_\eta z)_\zeta - (x_\zeta z)_\eta\}y]_\tau \left. \right\}/6. \end{aligned} \quad (19)$$

where *(Sym-cons-met.)* denotes *symmetric conservative metrics*. Similar symmetry property has been introduced to spatial metrics in conservative form by Vinokur and Yee[14]. The other time metrics are similarly expressed in *(Sym-cons-met.)*, but omitted for brevity.

The spatial metrics are expressed as

$$\xi_z/J = (x_\eta y)_\zeta - (x_\zeta y)_\eta, \quad \eta_z/J = (x_\zeta y)_\xi - (x_\xi y)_\zeta, \quad \zeta_z/J = (x_\xi y)_\eta - (x_\eta y)_\xi, \quad (20)$$

with which the discretized SCL identities are satisfied for any linear high-order finite difference scheme. The other spatial metrics in Eq.(4) are similarly rewritten. These expressions were first introduced by Thomas and Lombard for a second-order central scheme [11] and were subsequently extended for any linear high-

order finite difference scheme experimentally by Gaitonde and Visbal (Sec. 8 in [6], Sec. 4.2 in [15]). The mathematical proof and extension to the symmetric form have been carried out by Vinokur and Yee (Sec. 8.3.3 in [14]). Note that all schemes in Sec. 4 adopt Eq.(20) as spatial metrics.

### 3.2 Discretization of asymmetric conservative metrics

In this section, the validation of the discretized *asymmetric conservative metrics* is performed in a manner similar to that for spatial metrics by Deng et al. [4]. Let  $\phi(\tau, \xi, \eta, \zeta)$  represent an arbitrary physical quantity in physical space, which is discretized as  $\phi(\tau_i, \xi_j, \eta_k, \zeta_l) \equiv \phi_{i,j,k,l}$ . We introduce the multiple finite difference operator as

$$\delta_1^\xi (\delta_2^\tau \phi)_{i,j,k,l} \simeq \frac{\partial}{\partial \xi} \left( \frac{\partial}{\partial \tau} \phi_{i,j,k,l} \right), \quad (21)$$

where the subscript of the finite difference operator  $\delta$  indicates the number of finite difference schemes, and the physical quantity is differentiated with respect to the variables denoted by the superscripts. The left hand side of the VCL identity is discretized with the finite difference operator (21) as follows:

$$\begin{aligned} & \delta_1^\tau (1/J) + \delta_1^\xi (\xi_t/J) + \delta_1^\eta (\eta_t/J) + \delta_1^\zeta (\zeta_t/J) \\ & = \delta_1^\tau (\delta_2^\zeta A + \delta_2^\eta B + \delta_2^\xi C) + \delta_1^\xi (\delta_2^\eta D + \delta_2^\zeta E - \delta_2^\tau C) \\ & \quad + \delta_1^\eta (\delta_2^\zeta F - \delta_2^\tau B - \delta_2^\xi D) + \delta_1^\zeta (-\delta_2^\tau A - \delta_2^\xi E - \delta_2^\eta F). \end{aligned} \quad (22)$$

Note that Eq.(22) is obtained by substituting (*Asym-cons-met.*) for time metrics and the Jacobian [Eqs.(15)–(17) and Eq.(14)] into the left hand side of the VCL identity (13). The symbols from  $A$  to  $F$  in Eq.(22) correspond to each term in time metrics [Eqs.(15)–(17)] and the Jacobian [Eq.(14)]. Here, the subscripts for the indices are omitted for brevity. The discretized VCL identity is satisfied [in other words, Eq.(22) diminishes] only when the following relationships are satisfied.

$$\delta_1^\tau \delta_2^\zeta = \delta_1^\zeta \delta_2^\tau, \quad \delta_1^\tau \delta_2^\eta = \delta_1^\eta \delta_2^\tau, \quad \delta_1^\tau \delta_2^\xi = \delta_1^\xi \delta_2^\tau, \quad (23)$$

$$\delta_1^\xi \delta_2^\eta = \delta_1^\eta \delta_2^\xi, \quad \delta_1^\xi \delta_2^\zeta = \delta_1^\zeta \delta_2^\xi, \quad \delta_1^\eta \delta_2^\zeta = \delta_1^\zeta \delta_2^\eta. \quad (24)$$

The relationships (23) and (24) are nontrivial. In the following,  $\delta_1^\tau \delta_2^\eta = \delta_1^\eta \delta_2^\tau$  represents the relationships (23) and (24). We show that  $\delta_1^\tau \delta_2^\eta = \delta_1^\eta \delta_2^\tau$  is satisfied for any linear high-order finite difference method under the following condition. Any linear high-order finite difference operator [4] can be described as a weighted average of the first-order forward-facing difference operator as

$$\delta_1^\tau = \sum_{m=L_a}^{M_a} a_m (\phi_{i+m+1,j,k,l} - \phi_{i+m,j,k,l}), \quad \delta_1^\eta = \sum_{m=L_b}^{M_b} b_m (\phi_{i,j,k+m+1,l} - \phi_{i,j,k+m,l}), \quad (25)$$

$$\delta_2^\tau = \sum_{m=L_c}^{M_c} c_m (\phi_{i+m+1,j,k,l} - \phi_{i+m,j,k,l}), \quad \delta_2^\eta = \sum_{m=L_d}^{M_d} d_m (\phi_{i,j,k+m+1,l} - \phi_{i,j,k+m,l}). \quad (26)$$

The limits  $L_a, \dots, L_d, M_a, \dots, M_d$ , and coefficients  $a_m, \dots, d_m$  vary depending on the finite difference scheme employed. The discretized operators  $\delta_1^\tau \delta_2^\eta$  and  $\delta_1^\eta \delta_2^\tau$  can be expanded using either of the linear high-order

finite difference operators (25) and (26) as follows.

$$\delta_1^\tau \delta_2^\eta = \sum_{m=L_a}^{M_a} \sum_{n=L_d}^{M_d} \{a_m d_n (\phi_{i+m+1,j,k+n+1,l} - \phi_{i+m+1,j,k+n,l} - \phi_{i+m,j,k+n+1,l} + \phi_{i+m,j,k+n,l})\}, \quad (27)$$

$$\delta_1^\eta \delta_2^\tau = \sum_{m=L_b}^{M_b} \sum_{n=L_c}^{M_c} \{b_m c_n (\phi_{i+m+1,j,k+n+1,l} - \phi_{i+m+1,j,k+n,l} - \phi_{i+m,j,k+n+1,l} + \phi_{i+m,j,k+n,l})\}. \quad (28)$$

The relationship  $\delta_1^\tau \delta_2^\eta = \delta_1^\eta \delta_2^\tau$  becomes true at least under the following condition: for any  $m$ ,

$$\{a_m = c_m, d_m = b_m, M_a = M_c, L_a = L_c, M_d = M_b, L_d = L_b\}. \quad (29)$$

The sufficient condition (29) indicates that for multiple finite differences in a specific direction (including the time derivative), the unique operator should be used. This condition is also satisfied for the boundary scheme if the boundary scheme is unique for the same direction and is not satisfied when a different operation is used for a different grid line in the same direction. For this sufficient condition, any linear high-order finite difference operator can be employed to discretize the differentiation in the time and space directions. A similar approach can be used for the relationships (23) and (24). Note that discretized time metrics and Jacobian in (*Sym-cons-met.*) are similarly proven to satisfy the VCL identity.

## 4 Numerical tests

The compressible Euler equations are computed to validate the new evaluation for time metrics and the Jacobian, i.e., (*Asym-cons-met.*) and (*Sym-cons-met.*).

### 4.1 Computational methods

In this section, we present schemes and numerical methods.

#### 4.1.1 Time discretization

The governing equation is written in Eq.(9), with which (*Asym-cons-met.*) [Eqs.(14)–(17)] are used for the discretization of time metrics and the Jacobian. On the other hand, the governing equation is also reformed into its nonconservative form in terms of the Jacobian (Sec. 3.3 in [16] and Sec. 4.3 in [15]), with which (*Non-cons-met.*) [Eqs.(5)–(8)] can be used for the discretization of time metrics and the Jacobian. These governing equations are called the *conservative form* [(*Cons.*)] and *split form* [(*Split.*)], respectively.

$$(\text{Cons.}) \quad (Q/J)_\tau = -RHS_{(Q/J)}, \quad (30)$$

$$(\text{Split.}) \quad Q_\tau = -J\{RHS_{(Q/J)} - Q[(\xi_t/J)_\xi + (\eta_t/J)_\eta + (\zeta_t/J)_\zeta]\}, \quad (31)$$

where Eq.(30) corresponds to Eq.(9) and  $RHS_{(Q/J)}$  denotes the right hand side of Eq.(9). Equation (31) corresponds to Eq.(30) using the VCL identity (13). Note that because of freestream preservation, (*Cons.*) [Eq.(30)] should be adopted with (*Asym-cons-met.*) or (*Sym-cons-met.*) [Eqs.(14)–(17) or Eqs.(14)–(19)] for time metrics and the Jacobian, whereas (*Split.*) [Eq.(31)] does not offer such an expression for time metrics and the Jacobian that satisfy the discretized VCL identity. In the following, all schemes adopt the two-stage rational Runge-Kutta method for time integration on the basis of Eq.(30) or (31).

#### 4.1.2 Schemes and deforming grid

Here, we introduce some schemes for the computation of compressible Euler equations in order to validate the new evaluation for time metrics and the Jacobian, i.e., (*Asym-cons-met.*) or (*Sym-cons-met.*) [Eqs.(14)–(17) or Eqs.(14)–(19)]. The following schemes are used.

- NCM-CF: (*Non-cons-met.*) [Eqs.(5)–(8)] are used for the discretization of time metrics and the Jacobian; (*Cons.*) [Eq.(30)] is used for the time discretization of the governing equation.
- ACM-CF: (*Asym-cons-met.*) [Eqs.(14)–(17)] are used for the discretization of time metrics and the Jacobian; (*Cons.*) [Eq.(30)] is used for the time discretization of the governing equation.
- NCM-SF: (*Non-cons-met.*) [Eqs.(5)–(8)] are used for the discretization of time metrics and the Jacobian; (*Split.*) [Eq.(31)] is used for the time discretization of the governing equation.
- SCM-CF: (*Sym-cons-met.*) [Eqs.(18)–(19)] are used for the discretization of time metrics and the Jacobian; (*Cons.*) [Eq.(30)] is used for the time discretization of the governing equation.

The numerical methods and conditions common to all schemes in Table 1 are as follows. The computation is performed for the compressible inviscid fluid in the cubic region, which deforms with time. The governing equation are the compressible Euler equations [Eq.(30) or (31)]. The fluid is assumed to be an ideal gas and the ratio of specific heat  $\gamma = 1.4$  is that of air. Periodic boundary conditions are adopted for the computational region.

The initial grid exists in  $-L_0/2 \leq x_0, y_0, z_0 \leq L_0/2$  and has a cubic shape. Grid points in each direction are located at the equally spaced discrete  $N_{\max}$  points, that is, the position of the grid point is expressed as  $(x_{0;j}, y_{0;k}, z_{0;l}) = (-L_0/2 + (j-1)\Delta x_0, -L_0/2 + (k-1)\Delta y_0, -L_0/2 + (l-1)\Delta z_0)$  [ $\Delta x_0 = \Delta y_0 = \Delta z_0 = L_0/(N_{\max} - 1), 1 \leq j, k, l \leq N_{\max}$ ]. The body-fitted coordinates  $(\xi, \eta, \zeta)$  are discretized as  $(\xi_j, \eta_k, \zeta_l) = [(j-1)\Delta\xi, (k-1)\Delta\eta, (l-1)\Delta\zeta]$ . Let  $\Delta\xi = \Delta\eta = \Delta\zeta = 1.0$ , which corresponds to each grid points  $(x_{j,k,l}, y_{j,k,l}, z_{j,k,l})$ . The grid deforms temporally and each grid point  $[x_{j,k,l}^{\text{rm}}(\tau), y_{j,k,l}^{\text{rm}}(\tau), z_{j,k,l}^{\text{rm}}(\tau)]$  moves randomly:

$$x_{j,k,l}^{\text{rm}}(\tau) = x_{0;j} + R \sin[\phi_{j,k,l}^{\text{rm}}(\tau)] \cos[\theta_{j,k,l}^{\text{rm}}(\tau)], \quad (32)$$

$$y_{j,k,l}^{\text{rm}}(\tau) = y_{0;k} + R \sin[\phi_{j,k,l}^{\text{rm}}(\tau)] \sin[\theta_{j,k,l}^{\text{rm}}(\tau)], \quad (33)$$

$$z_{j,k,l}^{\text{rm}}(\tau) = z_{0;l} + R \cos[\phi_{j,k,l}^{\text{rm}}(\tau)], \quad (34)$$

where  $R = 0.20\Delta x_0$  and  $-\pi/2 \leq \theta_{j,k,l}^{\text{rm}}(\tau), \phi_{j,k,l}^{\text{rm}}(\tau) \leq \pi/2$  are given randomly. The computational parameters are set as follows:  $\Delta x_0 = 0.1$ ,  $N_{\max} = 21$ , and  $\Delta\tau = 0.1$ , i.e., the Courant number is set to 0.37. The computation is performed for  $0 \leq \tau \leq 6.0$ , and the computational time is discretized as  $\tau_n = n\Delta\tau$ . Note that the manner of grid deformation is consistent for each numerical test (in Sec. 4.2.1 and Sec. 4.2.2).

Table 1: Schemes examined in this paper

Scheme	Time metrics and the Jacobian	Governing equations
NCM-CF	( <i>Non-cons-met.</i> ) [Eqs.(4)–(5)]	( <i>Cons.</i> ) [Eq.(30)]
ACM-CF	( <i>Asym-cons-met.</i> ) [Eqs.(14)–(17)]	( <i>Cons.</i> ) [Eq.(30)]
SCM-CF	( <i>Sym-cons-met.</i> ) [Eqs.(18)–(19)]	( <i>Cons.</i> ) [Eq.(30)]
NCM-SF	( <i>Non-cons-met.</i> ) [Eqs.(4)–(5)]	( <i>Split.</i> ) [Eq.(31)]

## 4.2 Computational results

### 4.2.1 Freestream preservation

Now, the error in freestream preservation is shown. The initial flow is assumed to be a uniform flow in the  $x$  direction:

$$u_0 = 0.10, \quad v_0 = w_0 = 0.0, \quad p_0 = \rho_0 = 1.0. \quad (35)$$

First,  $L_\infty$ -norm is defined as the maximum disturbance of the flow velocity at  $\tau = 6.0$ :  $L_\infty \equiv \max\{|v - v_0|/u_0, |w - w_0|/u_0\}$ . The preservation of conservative quantities integrated over the computational region

is also defined as

$$\hat{\phi} \equiv \phi/J, \quad (36)$$

$$\langle \phi \rangle \equiv \sum_{j,k,l=1}^{N_{\max}} (\hat{\phi} - \hat{\phi}_0)_{j,k,l} / \sum_{j,k,l=1}^{N_{\max}} \hat{\phi}_{0;j,k,l} \simeq \int_{\mathbf{V}_R} (\phi - \phi_0) d\mathbf{V} / \int_{\mathbf{V}_R} \phi_0 d\mathbf{V}, \quad (37)$$

where subscript 0 denotes the initial values and  $\mathbf{V}_R$  indicates the computational region. Table 2 shows the result of freestream preservation at  $\tau = 6.0$ , where the randomly deforming grid is used, and the fourth-order explicit central scheme is employed for the spatial discretization without losing generality.

Table 2 indicates that the schemes which satisfy discretized GCL identities, i.e., ACM-CF, SCM-CF and NCM-SF, maintain freestream preservation. The schemes where the conservative form of the governing equation is used, i.e., NCM-CF, ACM-CF and SCM-CF, maintain the preservation of the conservative quantities  $\langle Q \rangle$ . The use of (*Cons.*) for the governing equation potentially ensures the preservation of conservative quantities. Note that when a larger number of grid points or larger distortion, e.g.,  $R = 0.25\Delta x$ , is adopted for the grid, qualitatively similar results are obtained in terms of freestream preservation and the preservation of conservative quantities.

Table 2: Freestream preservation errors for randomly deforming grid ( $L_\infty$ -norm and  $\langle Q \rangle$  at  $\tau = 6.0$ ); fourth-order explicit central scheme is used.

Scheme	$L_\infty$ -norm	$\langle \rho \rangle$	$\langle \rho u \rangle$	$\langle \rho e \rangle$
NCM-CF	$5.00 \times 10^{-1}$	$6.72 \times 10^{-17}$	$1.14 \times 10^{-16}$	$3.04 \times 10^{-16}$
ACM-CF	$1.27 \times 10^{-15}$	$5.97 \times 10^{-17}$	$1.16 \times 10^{-16}$	$2.94 \times 10^{-16}$
SCM-CF	$8.03 \times 10^{-16}$	$3.16 \times 10^{-17}$	$1.02 \times 10^{-16}$	$2.63 \times 10^{-16}$
NCM-SF	$1.51 \times 10^{-15}$	$-6.44 \times 10^{-6}$	$-6.44 \times 10^{-6}$	$-6.44 \times 10^{-6}$

#### 4.2.2 Preservation of isentropic vortex

The initial flow is a two-dimensional isentropic vortex [3]:

$$u_0 = \varepsilon \frac{y}{R_c^2} \exp \left[ \alpha \left( 1 - \frac{x^2 + y^2}{R_c^2} \right) \right], \quad v_0 = \varepsilon \frac{x}{R_c^2} \exp \left[ \alpha \left( 1 - \frac{x^2 + y^2}{R_c^2} \right) \right], \quad (38)$$

$$T_0 = \frac{p_\infty}{\rho_\infty} - \frac{\gamma - 1}{4\alpha\gamma} \varepsilon^2 \exp \left[ 2\alpha \left( 1 - \frac{x^2 + y^2}{R_c^2} \right) \right], \quad (39)$$

$$w_0 = 0.0, \quad p_\infty = \rho_0 = \rho_\infty = 1.0, \quad (40)$$

where  $\varepsilon = 0.02$ ,  $\alpha = 0.204$ , and  $R_c = 1.0$ .

Figures 1, 2, 3 show contours of the velocity magnitude on the  $\zeta$ -constant plane at  $\tau = 6.0$  for a randomly deforming grid with a fourth-order explicit central scheme. Figure 4 shows the distribution of  $v$ ,  $\rho$  and  $p$  along the  $\zeta$ - and  $\eta$ -constant line. The analytical solutions of  $v$ ,  $\rho$ , and  $p$  in Fig. 4 appear to be unfamiliar because they are calculated along the  $\zeta$ - and  $\eta$ -constant line, which is not straight at  $\tau = 6.0$ . Figures 1, 2, 3 and 4 indicate that the schemes that satisfy the discretized GCL identities, i.e., ACM-CF, SCM-CF and NCM-SF, maintain a vortex that is better than NCM-CF. In particular, SCM-CF shows the best resolution of a vortex in Figs. 1(a)–(d); it follows that on highly deforming grid, a vortex is better preserved by introducing the symmetry property into time metrics and Jacobian.

Figures 5(a) and (b) show the preservation of conservative quantities when the randomly deforming grid is used with the fourth-order explicit central scheme. Figures 5(a) and (b) indicate that NCM-CF, ACM-CF and SCM-CF preserve the conservative quantities that are integrated over the computational region. In addition, the preservation of the inverse of the Jacobian integrated over the computational region, i.e., the volume of the computational region, is better with ACM-CF and SCM-CF than with SDM-CF and SDM-SF [see Fig. 5(c)]. In particular, the use of (*Cons.*) for the governing equation potentially ensures the

preservation of conservative quantities, which is a result similar to that of freestream preservation (shown in Table 2). We also computed the isentropic vortex on a sinusoidally deforming grid and confirmed that the formal order-of-accuracy is maintained by checking the  $L_2$ -error while varying the grid density.

Note that when *asymmetric conservative metrics* are adopted for the random grid with  $R = 0.12\Delta x$ , the sixth-order compact scheme[7] blows up at  $\tau = 3.0$ ; on the other hand, *symmetric conservative metrics* does not blow up at  $\tau > 20.0$ . This indicates that the *symmetric conservative metric* is more robust for computations on an intensively deforming grid.

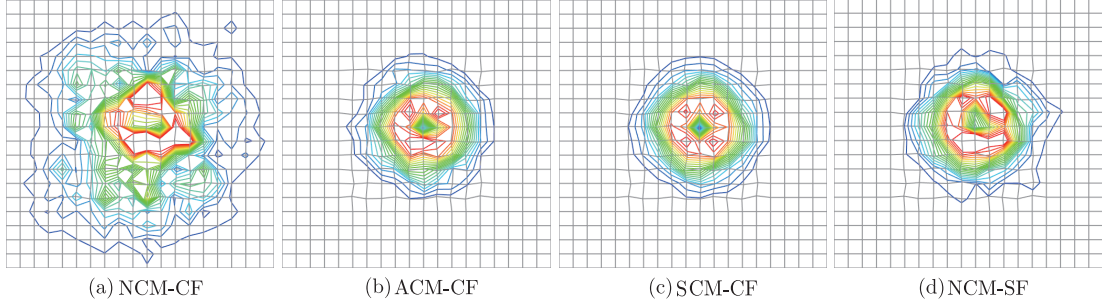


Fig. 1: Resolution of isentropic vortex (contours of velocity magnitude on  $\zeta$ -constant plane at  $\tau = 6.0$  on randomly deforming grid. Contour is from 0.0 to 0.34. The fourth-order explicit central scheme is employed for spatial discretization): (a) NCM-CF, (b) ACM-CF, (c) SCM-CF, (d) NCM-SF.

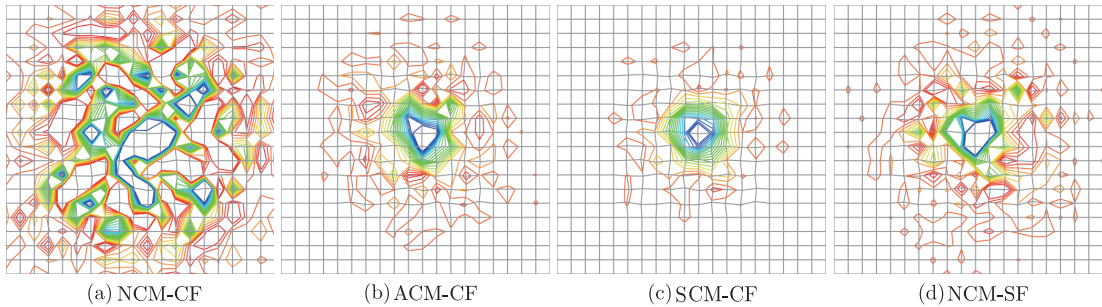


Fig. 2: Resolution of isentropic vortex (contours of pressure on  $\zeta$ -constant plane at  $\tau = 6.0$  on randomly deforming grid. Contour is from 0.85 to 1.02. The fourth-order explicit central scheme is employed for spatial discretization): (a) NCM-CF, (b) ACM-CF, (c) SCM-CF, (d) NCM-SF.

## 5 Concluding remarks

A new evaluation for time metrics and the Jacobian, i.e., *asymmetric conservative metrics* and *symmetric conservative metrics* were investigated. It was shown that discretized *asymmetric* and *symmetric conservative metrics* satisfy the VCL identity with any linear high-order finite difference scheme. The new scheme with the use of *asymmetric* and *symmetric conservative metrics* for time metrics and the Jacobian accomplishes the both of preservation of freestream and the conservative quantities integrated over the computational region even on severely-deforming grid. In particular, *symmetric conservative metrics* where a symmetry property in space is introduced into *asymmetric conservative metrics* give fine resolution for the computation of a vortex.

Numerical tests were conducted to validate this new evaluation for time metrics and the Jacobian: the computation of compressible Euler equations was performed for a three-dimensional randomly deforming grid, where freestream preservation and the resolution of a two-dimensional isentropic vortex were examined. When the fourth-order explicit central scheme was employed for spatial discretization on a randomly deforming grid, in terms of freestream preservation, the performance of the schemes with *asymmetric* and

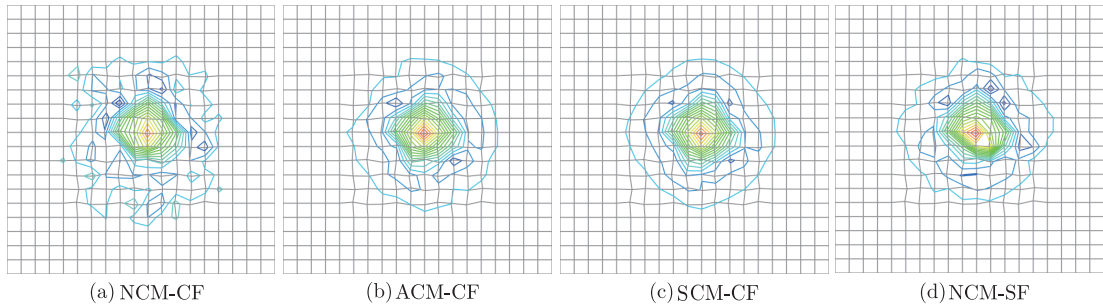


Fig. 3: Resolution of isotropic vortex (contours of  $z$ -vorticity on  $\zeta$ -constant plane at  $\tau = 6.0$  on randomly deforming grid. Contour is from 0.0 to 0.34. The fourth-order explicit central scheme is employed for spatial discretization): (a) NCM-CF, (b) ACM-CF, (c) SCM-CF, (d) NCM-SF.

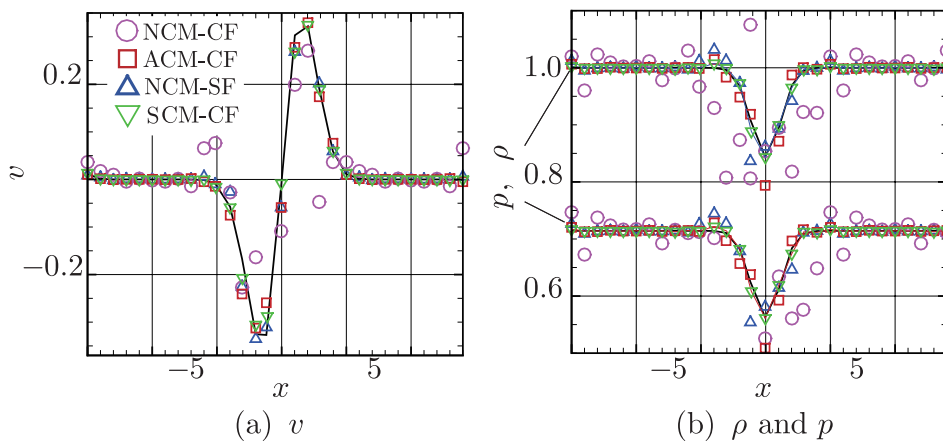


Fig. 4: Resolution of isotropic vortex (the distribution of  $v$ ,  $\rho$  and  $p$  along  $\zeta$ - and  $\eta$ -constant line at  $\tau = 6.0$  on a randomly deforming grid. A fourth-order explicit central scheme is employed for spatial discretization): (a)  $v$ , (b)  $\rho$  and  $p$ .

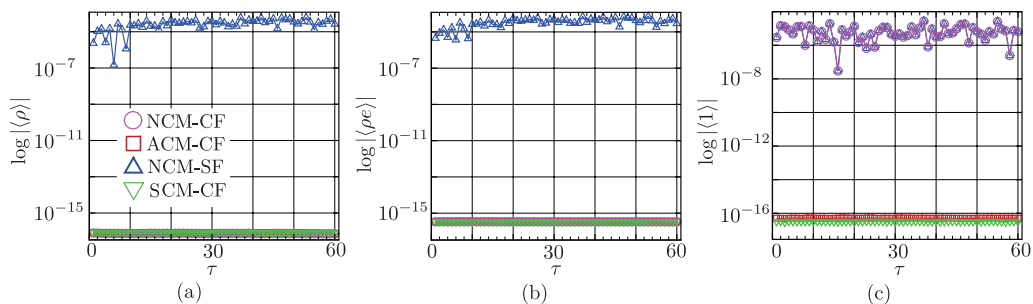


Fig. 5: Preservation of conservative quantities and inverse of the Jacobian (fluctuation of  $\langle \phi \rangle$  in the  $\tau$ -direction. The fourth-order explicit central scheme is employed for spatial discretization.  $\log |\langle 1 \rangle|$  corresponds to the error in conservation of the inverse of the Jacobian): (a)  $\log |\langle \rho \rangle|$ , (b)  $\log |\langle \rho e \rangle|$ , (c)  $\log |\langle 1 \rangle|$ .

*symmetric conservative metrics* was similar to the widely used method, i.e., the *split form* (Sec. 3.9 in [5], Sec. 3.1 in [9], Sec. 4.3 in [15] and Sec. 3.3 in [16]) of the governing equation. However, the preservation of conservative quantities integrated over the computational region can be achieved only when the *conservative form* of the governing equation is adopted, with which the use of *asymmetric* and *symmetric conservative metrics* for time metrics and the Jacobian preserves the freestream. When the sixth-order compact scheme [7] was employed, the preservation of conservative quantities should be carefully considered. This is because all inner points evaluated by the compact scheme are influenced by the boundary scheme, and the conservation property has a strong relationship with the inflow and outflow at the boundary. With respect to the resolution of the two-dimensional isentropic vortex, there was no significant difference between the two evaluations for time metrics and the Jacobian: *nonconservative metrics* and *asymmetric conservative metrics*. However, with introducing the symmetry property into *asymmetric conservative metrics*, i.e., using *symmetric conservative metrics*, the resolution of isentropic vortex was improved on intensively deforming grid. The preservation of conservative quantities was also significantly improved with the *asymmetric* and *symmetric conservative metrics*. Therefore, we conclude that in terms of freestream preservation and the resolution of the isentropic vortex, the discretized VCL identity should be satisfied with any scheme i.e., the use of *asymmetric* and *symmetric conservative metrics* for time metrics and the Jacobian or the use of the *split form* of the governing equation. On the other hand, the preservation of conservative quantities integrated over the computational region is maintained only when the *conservative form* of the governing equation is used (see Table 3). In terms of the improvement of resolution for an isentropic vortex on highly-deforming grid, the symmetry property in space for time metrics and Jacobian was considered to be of great significance. In addition, *symmetric conservative metrics* is more robust than *asymmetric conservative metrics* with the use of sixth-order compact scheme. The robustness of the *symmetric conservative metrics* is pursued in terms of their geometries in present: for example, it was determined that the discretized Jacobian based on the *symmetric conservative metric* corresponds to the volume of the cell with any linear high-order finite difference scheme [1][2].

Table 3: Summary of schemes;  $\circ$  is better than  $\times$ ;  $\odot$  is better than  $\circ$ .

Scheme	Preservation of conservative quantities	Freestream preservation	Resolution of vortex
NCM-CF	$\circ$	$\times$	$\times$
ACM-CF	$\circ$	$\circ$	$\circ$
SCM-CF	$\circ$	$\circ$	$\odot$
NCM-SF	$\times$	$\circ$	$\circ$

## References

- [1] Y. Abe, N. Iizuka, T. Nonomura and K. Fujii, “Geometries of Discretized Symmetric-conservative Metric Evaluations for Higher-order Finite Difference Scheme,” to be presented in the 23rd International Congress of Theoretical and Applied Mechanics, 2012.
- [2] Y. Abe, T. Nonomura, N. Iizuka and K. Fujii, “On the Discretization of Spatial Metrics Satisfying the GCL identities,” to be presented in the 6th European Community on Computational Methods in Applied Sciences, 2012.
- [3] D.S. Balsara and C.W. Shu, “Monotonicity Preserving Weighted Essentially Non-oscillatory Schemes with Increasingly High Order of Accuracy,” *J. C Phys.*, **160** (2000), 423–425.
- [4] X. Deng, M. Mao, G. Tu and H. Zhang, “Geometric conservation law and applications to high-order finite difference schemes with stationary grids,” *J. C Phys.*, **230** (2011), 1103–1105.
- [5] John A. Ekaterinaris, “High-order accurate, low numerical diffusion methods for aerodynamics” *Progress in Aero. Sci.*, **41** (2005), 192–300.
- [6] D.V. Gaitonde and M.R. Visbal, “Further development of a Navier-Stokes solution procedure based on higher-order formulas,” *AIAA Paper 99-0557* (1999), 1–52.

- [7] S.K. Lele, “Compact Finite Difference Scheme with Spectral-Like Resolution,” *J. C Phys.*, **103** (1992), 16–22.
- [8] T. Nonomura, N. Iizuka and K. Fujii, “Freestream and vortex preservation properties of high-order WENO and WCNS on curvilinear grids,” *C. Fluids*, **39** (2010), 197–214.
- [9] K. Okada, A. Oyama, K. Fujii and K. Miyaji, “Computational Study of Effects Nondimensional Parameters on Synthetic Jets” *Trans. Japan Soc. Aero. Space Sci.*, **55** (2012), 1–11.
- [10] T.H. Pulliam and J.L. Steger, “On Implicit Finite-Difference Simulations of Three Dimensional Flow,” *AIAA*, **10** (1978).
- [11] P.D. Thomas and C.K.Lombard, “Geometric Conservation Law and Its Application to Flow Computations on Moving Grids,” *AIAA Journal*, **17** (1979), 1030–1034.
- [12] M. Vinokur “Conservation Equations of Gasdynamics in Curvilinear Coordinate Systems,” *J. C Phys.*, **14** (1974), 105–125.
- [13] M. Vinokur, “An Analysis of Finite-Difference and Finite-Volume Formulations of Conservation Laws,” *J. C Phys.*, **81** (1989), 1–52.
- [14] M. Vinokur and H.C. Yee, “Extension of efficient low dissipation high-order schemes for 3-D curvilinear moving grids,” *World Scientific, Frontiers of computational fluid dynamics 2002*, 129–164.
- [15] M.R. Visbal and D.V. Gaitonde, “On the Use of Higher-Order Finite-Difference Schemes on Curvilinear and Deforming Meshes,” *J. C Phys.*, **181** (2002), 155–185.
- [16] M.R. Visbal and R.E. Gordnier, “A High-Order Flow Solver for Deforming and Moving Meshes,” *AIAA Paper 2000–2619*, (2000).
- [17] H. Zhang, M. Reggio, J.Y. Trepanier and R. Camarero, “Discrete Form of the GCL for Moving Meshes and its Implementation in CFD Schemes,” *C. Fluids*, **22** (1993), 9–23.